Phantom Based Point by Point Photon Counting and Imaging of Human Skin Tissue[1,2]

B. Jalil[a], O. Salvetti[a], M. Righi[a], L. Poti[b], and A. L'Abbate[c]

[a] *Istituto di Scienza e Tecnologie dell'Informazione "Alessandro Faedo" CNR, Pisa, Italy*

[b] *Consorzio Nazionale Interuniversitario per le Telecomunicazioni, CNR, Pisa, Italy*

[c] *Istituto di Fisiologia Clinica CNR, Pisa, Italy*

e-mail: Ovidio.Salvetti@isti.cnr.it, Bushra_jalil@hotmail.com

Abstract—Time-correlated single photon counting (TCSPC) is popular in the resolved techniques due to its prominent performance such as ultra-high time resolution and ultra-high sensitivity. This paper presents advance signal processing techniques on the optical TCSPC signals obtained from the series of experiments on fabricated tissue like phantom. A pulsed laser sources at a wavelength of 830 rim transmits the light through the surface of phantom and finally at receiver side, photon counting device generates the histogram of the receiving signal. The noisy data obtained from the photon counter is processed with the splitting based denoising method. The method divide the signal into different subsets based on the transitions. Each subset is then processed individually and final merging of all subsets gives noise free signal. The main objective of this work is to analyze the signal obtained from photon counter in context of skin blood absorption. We had examined the signal obtained by varying the distance between transmitter and receiver to extract the features. Experimental results with our prototype shows more scattering with the increase in the distance at 3dB level and hence less absorption with increase in the distance.

Keywords: time-correlated single photon counting (TCSPC), phantom based experiment, skin tissue, denoising, Wavelet transform based spitting, transmitter receiver distance.

DOI: 10.1134/S1054661816010107

1. INTRODUCTION

There is a rapid growth of TCSPC based image processing applications in different aspects of science e.g., meterology, architecture and more prominently in medical and defense applications. The main interest in optical techniques for imaging through scattering has been motivated by the desire to develop a more effective, less expensive, and safer alternative to X-ray. Amann et al. has reviewed some of these application in their work [1]. Similarly, Wallace et al. has studied time correlated single photon counting in terms of 3D imaging [2]. Among several of these applications, assessment of breast cancer has been extensively advanced and studied for the assessment of breast physiology and pathology. Taroni et al. [3, 4] has presented their finding and similarly Zhang et al. [5] have also presented their experimental finding for medical application. These time resolved techniques measure time-dependent transmittance, reflectance, and fluorescence in response to illumination by an ultrashort light pulse. Two good examples are time-resolved diffuse optical tomography and fluorescence lifetime imaging. Both techniques require measurements in the time domain, in which short excitation pulses are used. With periodic excitation, e.g., from a laser, it is possible to extend the data collection over multiple cycles of excitation [2]. In general, a laser is directed towards the target and a single photon detection system is triggered by scattered optical return and each photon return is termed as an independent measurement of the photon return [6, 7]. Becker has explained in detail the principle and applications of TCSPC systems more specifically in imaging [7]. The collection of multiple returns result in time measurements. These techniques often suffer from high noise due to the time duration of measurement and the low optical signal. For that reason, averaging is required. In order to reduce the noise the number of acquisition gets higher and higher making the system time consuming and sensitive to time drift. In this work we have used advanced signal processing methods to reduce impact of noise for each individual acquisition in order to reduce both the number of acquisition and the time. Furthermore, we have used advanced signal processing methods to investigate the signal acquired from such systems.

[1] This paper uses the materials of the report submitted at the 9th Open German-Russian Workshop on Pattern Recognition and Image Understanding, held in Koblenz, December 1–5, 2014 (OGRW-9-2014).

[2] The article is published in the original.

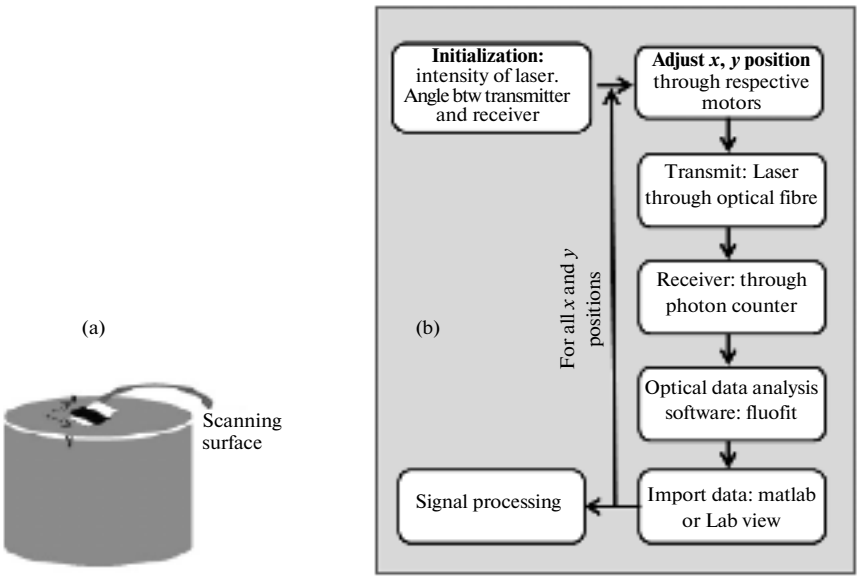

Fig. 1. (a) Phantom based experiment. Black line on the surface blocks the photons to pass through the surface and result in reducing the peak of the histogram of photon counts, (b) flow chart of the data acquisition method.

1.1. Experimental Setup

In this work, wo propose to study the penetration of a pulsed laser light on human skin tissues in case of normal and pathological situation. In order to explore this application, we had conducted phantom, shown in Fig. 1a based experiments. The fabricated tissue like solid phantom mimics the real human skin. A solid plastic phantom has been developed with optical properties that closely match those of human skin tissues. The flow chart of the complete processing is illustrated in Fig. 1b. After initialization of the laser source (Pico quant 830 nm laser source [8]), the transmitter (T_x) and receiver (R_x) moved in the x and y directions (with the help of two motors) to scan the surface. Each 1D signal belongs to the respective (x, y) position. The scanning time of each measurement was 20 s set at the constant rate. The obtained signal is further denoised with the splitting based algorithm explained in Section 2. Afterword, the extraction of parameters and retrieved information is finally explained in Sections 3 and 4.

2. DENOISING

In order to reduce number of acquisition, we had applied advanced signal processing to remove noise elements. In order to do so. several algorithm based on wavelet transform has been proposed in the past. However, very few of them discussed about the singularities or interruptions present inside the signal [9]. The main objective of these methods is to extract the noise free signal, but not on preserving the energy at the edges. In this work, we will examine the absorption scattering by changing the distance between T_x and R_x with respect to the peak of photon counting histogram. Recently, Jalil et al. proposed a denoising method based on splitting of the signal while preserving peak energy of the signal [10]. In order to achieve our objectives, we had applied the splitting based denoising in order to preserve the peak amplitude.

2.1. Principle of the Method

In order to estimate the noise free function F, the method splits the function Y into its subsets in spatial domain on the basis of the sharpness of transitions or edges such that:

$$Y \supseteq Y_{i = 1, 2, \ldots, J}, \quad (1)$$

Y denotes the set of all samples and each subset Y_i, with $i = 1,\ldots, J$ contains K_i adjacent samples $y_{i, l}$ with $l \in 1,\ldots K_i$. J is the total number of subset, and K_i is the length of the respective subset. Piecewise analysis has been performed on each subset of the function Y individually by following the algorithm as follows.

1. Wavelet transform based multiscale analysis was performed on each subset to extract modulus maxima across successive scales. These modulus maxima correspond to the transitions at that scale. The extraction of these modulus maxima results in generating modulus maxima lines. These lines were generated by tracing the maxima from coarser to finer scales. However since they suffer from the problem of delocalization

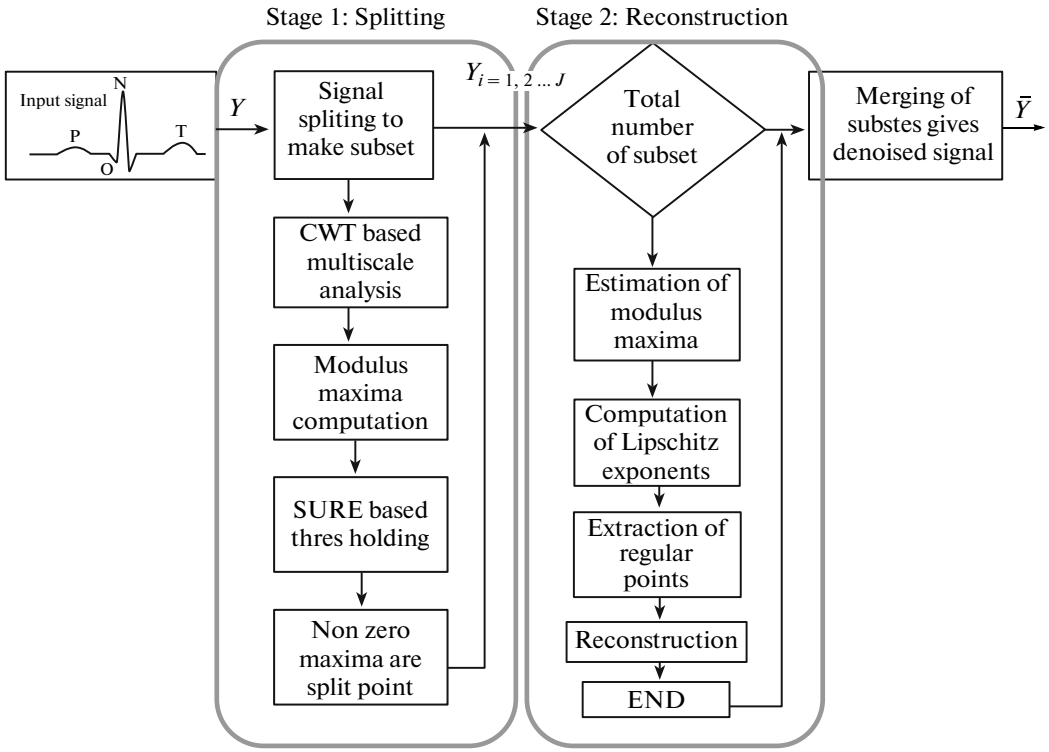

Fig. 2. Block diagram of the splitting based denoising algorithm. Mainly two stages (i) splitting and (ii) reconstruction. Final merging of all reconstructed subsets gives complete denoised signal.

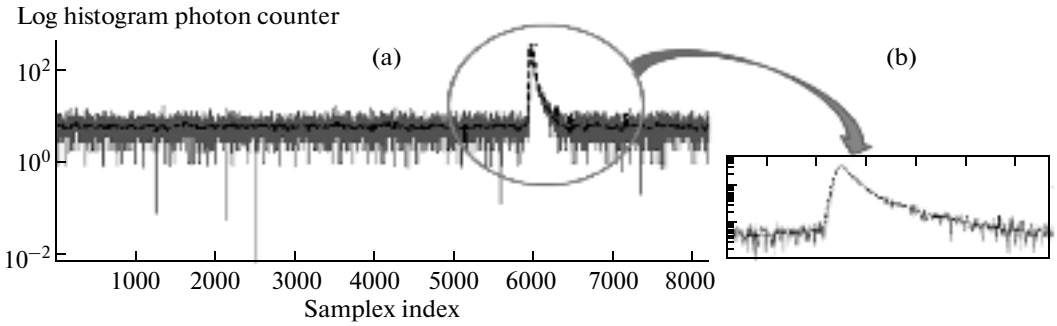

Fig. 3. Results obtained with denoising algorithm. (a) Solid lines shows noisy signal and dotted shows denoised signal. Also it can be observed from (b) that the denoising method has not altered the peak of the signal.

and in order to avoid this problem we traced the lines from finer to coarser scales.

2. Lipschitz exponents were computed from these maxima lines. These exponents in each subset identified regular or smooth points in respective subset. The regular point correspond to the positive Lipschitz exponents. They actually represents the order of differentiability of the point or signal.

3. After computing these exponents, the next step is reconstruction. The reconstruction of each subset is toration method between regular data samples (extracted on the basis of Lipschitz exponents) utilizes all sampled points and the smoothness of each subset to estimate the best fit. At the final stage, merging of all reconstructed subsets result in giving fully denoised signal. We define $y_{l=1,\ldots N} \in Y$

$$y_{i,l}^{k+1} = y_{i,l}^{k} + \lambda_i^k\left(-\frac{\partial C_i^{MSE,k}}{\partial y_{i\ l}}\right) + \gamma_i^k\left(-\frac{\partial C_i^{MSO,k}}{\partial y_{i\ l}}\right), \qquad (2)$$

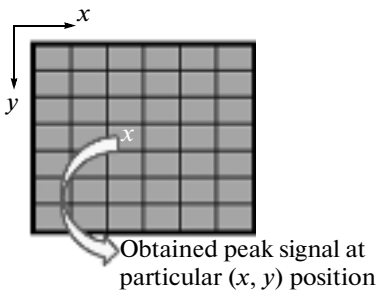

Fig. 4. Generating 2D map.

where $i = 1, ..., J$ and $y_{i,l}$ with $l \in 1, ... N_i$ adjacent samples in each subset, k define the iteration step, C_i^{MSE} is the mean square error estimation of the restored subset with the original signal of respective subset (y_{oi}).

Figure 3 shows the obtained signal after denoising. It can be observed from Fig. 3b that the signal has maintained its peak after denoising. In the next section, we will use the peak of the signal to extract the useful information about the skin tissue.

3. LESION EXPERIMENT

At the first stage, we had conducted induced lesion experiments. We had intentionally marked the black line on the surface of the phantom to block the light penetration on the surface and deep layers which represents the blockage on the surface of the skin due to lesions shown in Fig. 6a. A successful screening method must distinguish these lesion from the surrounding healthy tissue. We had defined the area around that lesion line as a window for point by point acquisition. The acquisition step was performed by moving transmitter and receiver (photon counter probe) x and y directions (with the help of two motors) to scan the surface. The complete surface was scanned point by point in horizontal and vertical directions. 2D maps generated in Matlab in context of peak signal is shown in Fig. 6.

We had used T-Cube DC Servo Controller (TDC001) to automatically control the movement of the source and receiver. Total of two motors were used to control the x and y movements for this experiment. Matlab based controlling software automatically adjusted the position of (T_x) and receiver (R_x) with an equal step size in both directions. Initially the constant 5 mm distance was maintained between T_x and R_x. Similarly, the scanning time for each acquisition was 20 s. The complete scan of a single row of the surface is shown in Fig. 5. It can be observed from the scanning results that, the area where there exist no black line result in allowing photons to pass through the surface arid correspond to the high amplitude of photon histogram reached at receiver end. On the other hand, low amplitude of the histogram correspond to either transmitter or receiver position on the boundary

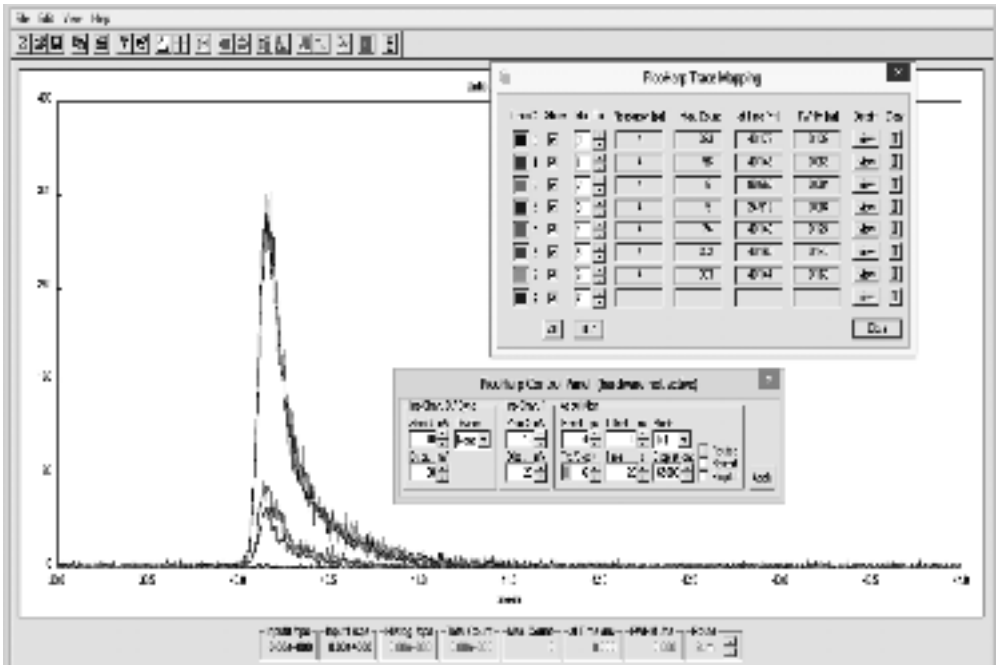

Fig. 5. 1D signal of the surface obtained with the Pico harp software. Single row scanning of the black line experiment.

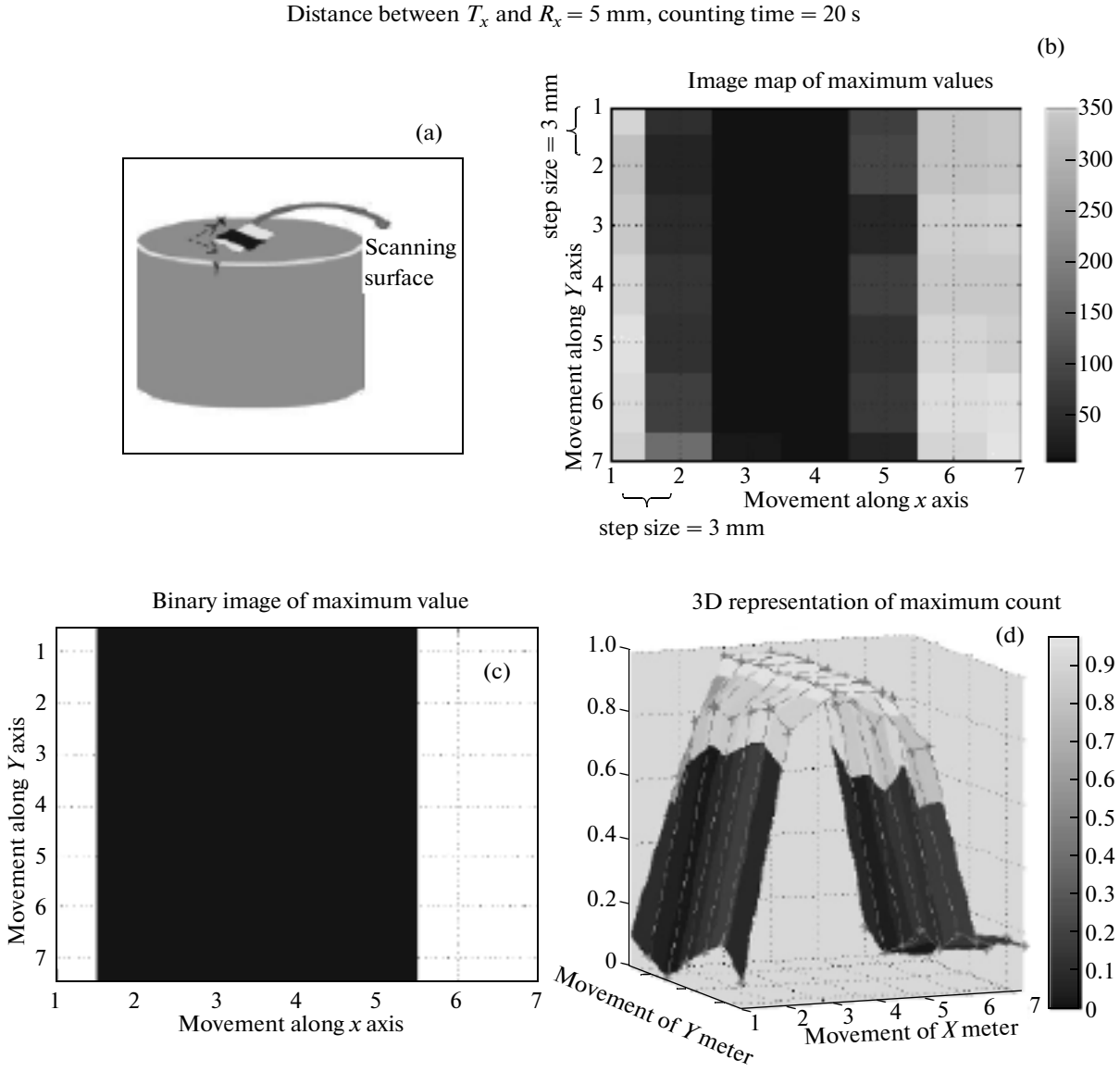

Fig. 6. Phantom based experiment. Black line on the surface blocks the photons to pass through the surface and result in reducing the maximum of the histogram of photon counts.

between two regions. The approximate zero max count of histogram correspond to the middle of the blockage area which does not allow photons to pass through the surface.

Once, we had obtained the complete scanning of the selected surface area with and without black lines. The next step was to generate 2D maps of the maximum counts of the histogram. The data was imported from pico harp software to Matlab and 2D map of the maximum values were generated as shown in Fig. 6b. The high intensity regions in the figure correspond to the surface which allows photons to pass through and gradually reaching the boundary of the blockage area (if move in x direction). As we reached at the boundary, the maximum counts reduces and reached at its minimum shown as black area. The maximum counts started to increase as reached again on the other side of the boundary and resume its counts while reaching the normal surface. In order to further classify the results, we binaries the map with the mean of the threshold value and the obtained map is shown in Fig. 6c where, black area correspond to very few maximum count of photons. The 3D view representing the max count value of the particular point is shown in Fig. 6d for better visualization and understanding.

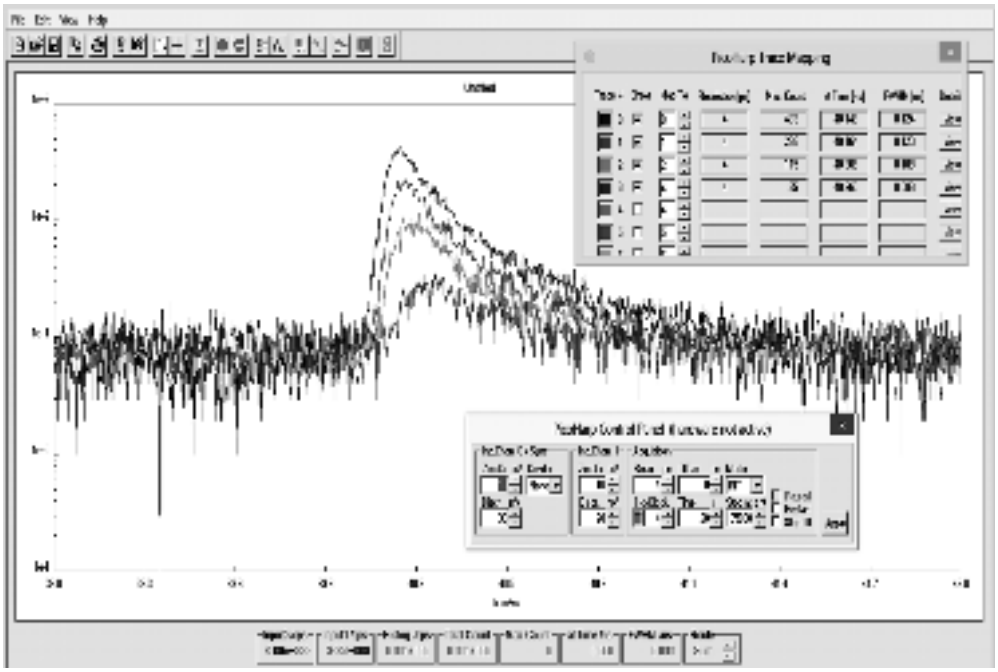

Fig. 7. Signal obtained at a point on the Pico harp software. Increase in the distance between T_x and R_x results in reducing the peak counts but increase in the pulse width.

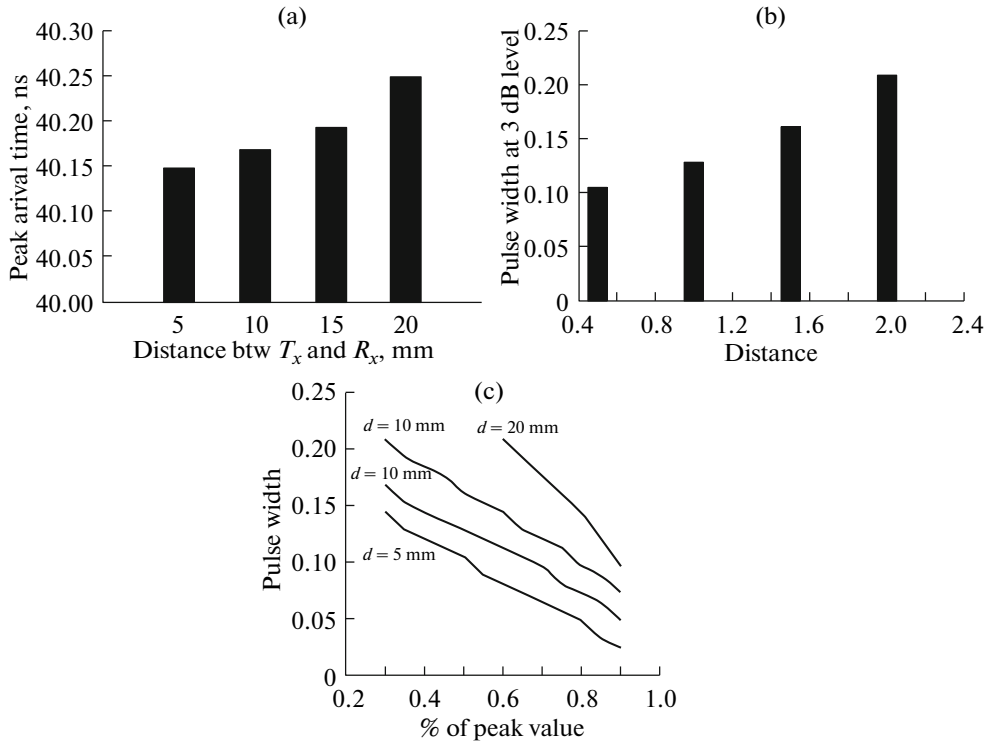

Fig. 8. Obtained features by varying the distance between T_x and R_x. (a) Histogram of peak arrival time, (b) histogram and curves at 3 dB, and (c) pulse width at different levels.

4. PROCESSING: VARYING DISTANCE BETWEEN T_x AND R_x

At the second stage, we had conducted the experiment at a single point on the surface of the phantom by varying the distance between transmitter and receiver. The data from the photon counting device is displayed on the provided Picoharp interface shown in Fig. 7. We had started with the minimum distance of 5 mm between the two (T_x and R_x) and then by increase with an equal step of 5 mm result in reducing the peak count to the half of the previous but more widening of pulse width. Trace 0 shows minimum distance. By invreasing the distance, the max counts of photons (Trace 1) reducing nearly half of the previous. However, it can be observed that the reaching time of the peak also slightly increase with the distance but was approximately within the range of 40 ns. At the second stage, we had estimated the width of the pulse at several levels by varying the distances. At 3 dB level, more widening of pulse width was observed by increasing in the distance and hence more scattering on the surface as shown in Fig. 8b. In Fig. 8c, curves at respective distance between T_x and R_x shows the pulse width at different level. Increase in the distance results in more scattering and hence less absorption. We can conclude from these findings that by varying the distance between T_x and R_x on the skin surface, we can approximately estimate the depth of the fluid on the level of the skin.

CONCLUSION

We had worked on the optical tomography techniques e.g., time correlated single photon counting methods. We had conducted phantom based experiments to analyze the fluid absorption on the human skin level. The hardware involved in these experiments includes Tlior labs Dc motors, Pico quant laser source and corresponding photon counting devices. Pico quant also provides external interface software to better visualize the results. The experiments includes surface scanning and analyzing the difference by varying the distance between T_x and R_x. By increasing the distance between T_x and R_x, the max counts of photons keep on reducing but increase in the pulse width. We conclude that the mean penetration depth of diffusively reflected photons depends on the distance between source and the detector.

ACKNOWLEDGMENTS

This work has been supported by Regione Toscana. Direzione Generale Competitività e Sviluppo Competenze. Area di Coordinamento della Ricerca.

REFERENCES

1. M. C. Amann, T. Bosch, M. Lescure, R. Myllylla, and M. Rioux, "Laser ranging: A critical review of usual techniques for distance measurement," Opt. Eng. **40** (1), 10–19 (2001).

2. G. S. Buller and A. M. Wallace, "Ranging and three-dimensional imaging using time-correlated single-photon counting and point-by-point acquisition," IEEE J. Selected Topics Quantum Electron. **13** (4), 1006–1015 (2007).

3. P. Taroni, A. Pifferi , G. Quarto, L. Spinelli, A. Torricelli, and F. Abbate, "Noninvasive assessment of breast cancer risk using time-resolved diffuse optical spectroscopy," J. Biomed. Opt. **15** (6), 060501 (2010).

4. P. Taroni, A. Pifferi, A. Torricelli, and R. Cubeddu, "Time-resolved optical spectroscopy and imaging of breast," Opto Electron. Rev. **12** (2), 249–253 (2004).

5. Qiang Zhang and Nan Guang Chen, "Pseudo-random single photon counting: the principle, simulation, and experimental results," in *Proc. SPIE 7170, Design and Quality for Biomedical Technologies II, 71700L* (February 23, 2009).

6. Weirong Mo and Nanguang Chen, "Fast time-domain diffuse optical tomography using pseudorandom bit sequences," Opt. Soc. Am. **16** (18), 13643–13650 (2008).

7. W. Becker, *Advanced Time-Correlated Single Photon Counting Applications* (Springer, 2015).

8. http://www.picoquant.com/

9. S. G. Mallat, *A Wavelet Tour of Signal Processing* (Acad. Press, 1999).

10. E. Fauvet, O. Laligant, and B. Jalil, "Signal restoration via a splitting approach," EURASIP J. Adv. Signal Processing **38**, (2012).